European Journal of Medicinal Chemistry xxx (2014) 1–13

Contents lists available at ScienceDirect

European Journal of Medicinal Chemistry

journal homepage: http://www.elsevier.com/locate/ejmech

Original article

Part I. Synthesis, biological evaluation and docking studies of new 2-furylbenzimidazoles as antiangiogenic agents

Ahmed Temirak [a], Yasser M. Shaker [a,*], Fatma A.F. Ragab [b], Mamdouh M. Ali [c], Hamed I. Ali [d,e], Hoda I. El Diwani [a]

[a] Department of Chemistry of Natural and Microbial Products, Division of Pharmaceutical and Drug Industries, National Research Centre, Dokki, 12622 Cairo, Egypt
[b] Department of Pharmaceutical Chemistry, Faculty of Pharmacy, Cairo University, Egypt
[c] Department of Biochemistry, Division of Genetic Engineering and Biotechnology, National Research Centre, 12622 Cairo, Egypt
[d] Department of Pharmaceutical Sciences, Irma Lerma Rangel College of Pharmacy, Texas A&M Health Science Center, TX, USA
[e] Department of Pharmaceutical Chemistry, Faculty of Pharmacy, Helwan University, Cairo, Egypt

ARTICLE INFO

Article history:
Received 8 September 2013
Received in revised form
24 January 2014
Accepted 31 January 2014
Available online xxx

Keywords:
2-(2-Furyl)-1H-benzimidazoles
Angiogenesis
Vascular endothelial growth factor (VEGF)
VEGFR2 kinase
Cytotoxicity

ABSTRACT

2-(2-Furyl)-1H-benzimidazoles **3**–**11** were synthesized and tested for their *in vitro* VEGF inhibition in MCF-7 cancer cell line. Compound **5a** was more potent than Tamoxifen, and compounds **3b**, **5a**, **5c**, **6b**, **7a** and **10** showed promising potency. Furthermore, compounds (**6b**, **7a** and **10**) showed remarkable selective inhibition of COX-2 enzyme close to that of Celecoxcib. Additionally, docking studies were performed using AutoDock 4.2 into the VEGFR2 kinase. Significant correlation exists between the biological activity (IC_{50} and %VEGF inhibition) against MCF-7 cell line and the molecular docking results (K_i and ΔG_b) with correlation coefficients (R^2) of 0.5513 and 0.4623 respectively. Accordingly, most of the synthesized 2-(2-furyl)-1H-benzimidazoles showed strong antiangiogenic activity against VEGFR2 kinase.

1. Introduction

Angiogenesis, new blood vessels formation, plays a central role in cancer cell survival, tumor growth which is considered as a precondition of metastasis for all solid tumors [1–3]. This process consists of the formation of new capillaries through splitting from pre-existing blood vessels. There are several growth factors involved in tumor angiogenesis which include vascular endothelial growth factor (VEGF) [4], basic fibroblast growth factor (bFGF) [5], epidermal growth factor (EGF) [6], platelet-derived growth factor (PDGF) [7] and angiopoietin Ref. [8]. Indeed, vascular endothelial growth factor (VEGF) is the most important signaling protein among the other growth factors that plays a vital role in stimulation of angiogenesis [9]. The VEGF family consists of six members of proteins (VEGF-A, B, C, D, E and placenta growth factor). These proteins can bind to their VEGF receptors (VEGFR1, VEGFR2 and VEGFR3). These receptors are belonging to receptor tyrosine kinases (RTK). VEGFR2 is considered as important receptor mediating of all the cellular responses to VEGF [10]. Binding of VEGF to its family of receptors (VEGFR), is the key mediator that promotes the proliferation and survival of endothelial cells and consequently cancer progression [11]. Therefore, looking for an effective anti-VEGF/VEGFR drug became the main interest for many research groups aiming to discover a new cancer therapy *via* angiogenesis inhibition.

Benzimidazole nucleus is of well known promising biological activity [12,13]. A series of 2-heteroaryl benzimidazole derivatives was discovered in literature as effective VEGF/VEGFR inhibitors for antiangiogenic tumor therapy. Fig. 1 includes selected 2-substituted benzimidazole structures as angiogenesis inhibitors. 2-Arylbenzimidazoles were reported as novel multi-target VEGFR2, EGFR and PDGFR kinases inhibitors [14]. 4-Amino-*N*-[2-[4-[(4-aminobenzoyl)amino]phenyl]-1H-benzimidazol-5-yl]benzamide **1** was discovered as a novel benzimidazole derivative with unique antiangiogenic characteristics that inhibited the vascular endothelial growth factor (VEGF) and basic fibroblast growth factor (bFGF)-induced growth of various endothelial cells without a cytotoxic phase [15]. A series of novel heterocyclic analogs 4-

* Corresponding author.
E-mail addresses: yabdelrahman@yahoo.com, yassershaker1972@yahoo.com (Y. M. Shaker).

0223-5234/$ – see front matter © 2014 Elsevier Masson SAS. All rights reserved.
http://dx.doi.org/10.1016/j.ejmech.2014.01.063

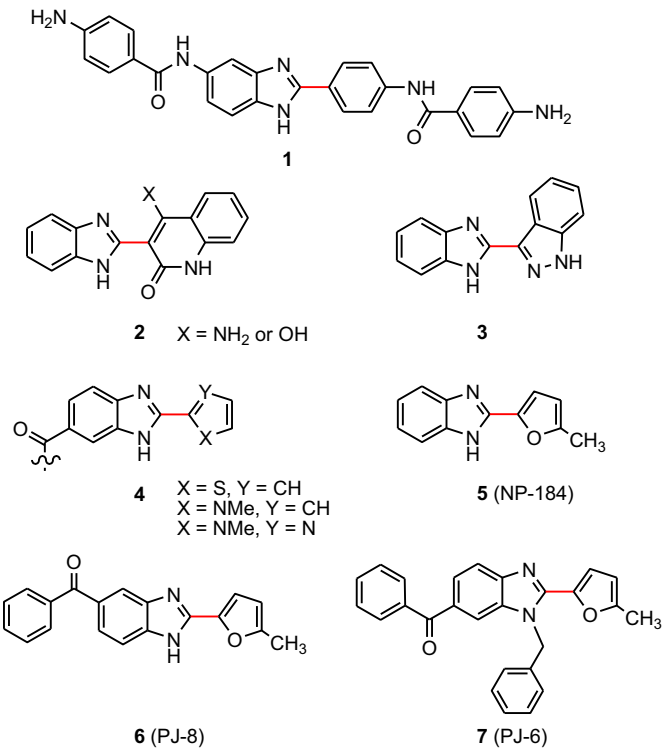

Fig. 1. Compounds **1**–**7**.

amino- or 4-hydroxy-3-benzimidazol-2-ylhydroquinolin-2-one **2** and 3-benzimidazol-2-yl-1H-indazole **3** was developed as potent VEGFR, FGFR, and PDGFR receptor tyrosine kinases (RTK) family inhibitors which represent an attractive therapeutic modality with interesting physicochemical and pharmacokinetic properties [16,17]. The DNA binding oligomers, incorporating benzimidazole ring substituted at position 2 with five membered heterocyclic ring **4**, was designed to target the hypoxia inducible factor (HIF-1α) binding site on the promoter of VEGF gene [18]. 2-(5-Methyl-2-furyl)-1H-benzimidazole (NP-184) **5** was discovered as a novel potential candidate for the treatment of angiogenesis related-diseases [19,20]. It was reported that NP-184, which exhibited a potent anti-thrombotic activity, inhibited several angiogenic functions of human umbilical vascular endothelial cells (HUVEC), including proliferation, migration and tube formation. In addition, NP-184 was discovered to reduce the angiogenesis *in vivo* in material plug assay model [19,20]. PJ-8, 5-benzoyl-2-(5-methyl-2-furyl)-1H-benzimidazole, **6** may function as a novel drug candidate in anticancer therapy because PJ-8 significantly inhibited VEGF–VEGFR2 and suppressed tumor-induced angiogenesis *in vivo* [21]. PJ-6, 6-benzoyl-1-benzyl-2-(5-methyl-2-furyl) benzimidazole, **7**, the close chemical analog of PJ-8, was also evaluated for its antiangiogenic activity through inhibiting cell proliferation and migration of endothelial cells. Indeed, PJ-8 was expected to be a novel candidate as an antiangiogenic agent [21].

Therefore, looking for derivatives of 2-(2-furyl)-1H-benzimidazole through modification and functionalization of the structure is an important point of research aiming to find analogs for the drug candidates 2-(2-furyl)-1H-benzimidazoles NP-184, **5**, and PJ-8, **6** for angiogenesis inhibition. In an effort to discover more effective VEGF/VEGFR inhibitors as antiangiogenic agents, we have designed, synthesized and evaluated a series of benzimidazole compounds in general and bearing 2-furyl substituent at the 2-position more specifically for their antiangiogenic activity. Our synthetic strategy of synthesizing new analogues was based through substitution at position 5 of the furyl ring at the right hand side (part **A**) and/or modification of the benzimidazole ring at the left hand side (part **B**) through the introduction of various heterocyclic ring systems at position 1 (Fig. 2).

The synthesized compounds **3**–**11** (Scheme 1) were tested for their antitumor activity against MCF-7 breast cancer cell lines and their *in vitro* inhibitory action against VEGFR kinase enzyme using double-antibody sandwich enzyme-linked immunosorbent assay (ELISA) to assay the level of human VEGF in breast cancer cell line MCF-7. These antiangiogenic studies were achieved in comparison to the reference drug, Tamoxifen which is reported as a potent inhibitor of angiogenesis [22].

Some recent researches have stated that there is a significant overexpression of cyclooxygenase-2 enzyme (COX-2) and VEGF in malignant tumors which contribute to an increase in angiogenesis *via* the activation of p38 and JNK kinase pathways [23,24]. Moreover, immunohistochemical studies have shown that COX-2 is strongly associated with increased angiogenesis and the increase in VEGF production [25]. Thus, study of the COX-2 selectivity inhibition of some of the compounds exhibiting excellent inhibition against human VEGF in human breast cancer cell line MCF-7 showed that they are highly potent and selective to COX-2 rather than COX-1.

Molecular docking studies of 2-(2-furyl)-1H-benzimidazole derivatives against receptor tyrosine kinase VEGFR2 (PDB code: 3EWH) [26] using AutoDock 4.2 and correlating the docking results with the *in vitro* inhibition against VEGF in human breast cancer cell line MCF-7 helped in deducing the structure activity relationship of the synthesized compounds as antiangiogenic VEGR2 inhibitors. Compound **5a** was found to be more potent than Tamoxifen against MCF-7 cell line as well as possessing better *in vitro* VEGF inhibition in human breast cancer than Tamoxifen and can be used as lead compound in the future.

2. Results and discussion

2.1. Chemistry

The target compounds **3**–**11** were synthesized according to the reaction sequences outlined in Scheme 1. 2-(Furan-2-yl)-1*H*-benzo[*d*]imidazole **3a** and its 5-methyl derivative **3b** were prepared according to the literature procedure [27–29] *via* the condensation of 1,2-phenylenediamine **1** with furfural **2a** or 5-methylfurfural **2b** in presence of *p*-toluenesulfonic acid/DMF. Reaction of **3a**,**b** with various chloro compounds was achieved in K_2CO_3/acetone at room temperature to form the N-substituted product **5a**–**c**. Under the same reaction conditions, treatment of the 1*H*-benzimidazoles **3a**,**b** with ethyl bromoacetate achieved the N-alkylated products **4a**,**b,** which were refluxed with hydrazine hydrate in ethanol to obtain the desired acid hydrazide compounds, 2-[2-(furan-2-yl)-1*H*-benzo[*d*]imidazol-1-yl]acetohydrazide **6a** and its 5-methyl derivative **6b** as the key compounds to form the desired target products **7**–**11** (Scheme 1).

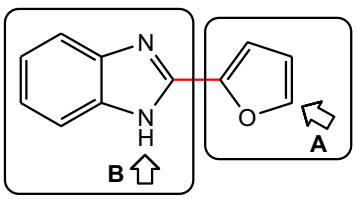

Fig. 2. Schematic diagram of the substitution positions on the lead compound.

Please cite this article in press as: A. Temirak, et al., Part I. Synthesis, biological evaluation and docking studies of new 2-furylbenzimidazoles as antiangiogenic agents, European Journal of Medicinal Chemistry (2014), http://dx.doi.org/10.1016/j.ejmech.2014.01.063

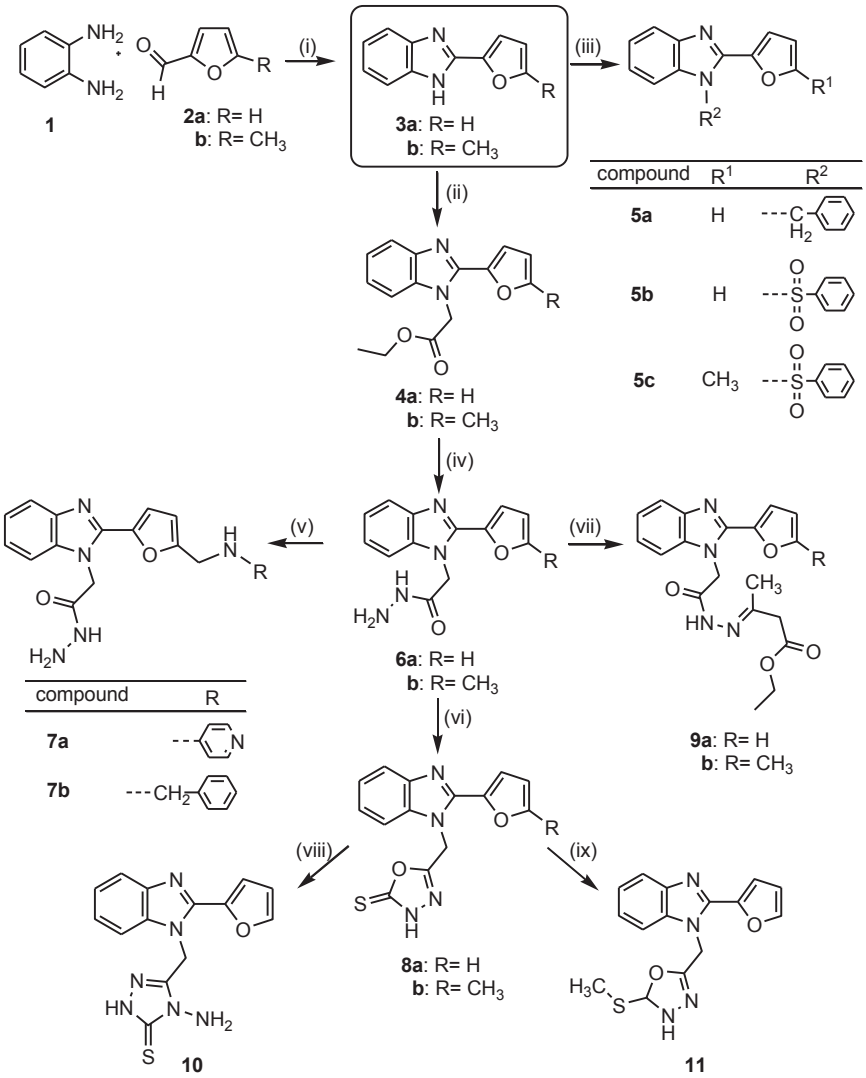

Scheme 1. Synthesis of compounds **3**–**11**. *Reagents and conditions*: (i) *p*-Toluenesulfonic acid, DMF, 100 °C; (ii) Ethyl 2-bromoacetate, K_2CO_3, acetone, R.T.; (iii) Chloro compounds, K_2CO_3, acetone, R.T.; (iv) Hydrazine hydrate, ethanol, 90 °C; (v) Primary amine, paraformaldehyde, ethanol, reflux; (vi) Carbon disulphide, KOH, ethanol, ice bath followed by reflux; (vii) Ethyl acetoacetate, KOH, ethanol, reflux; (viii) Hydrazine hydrate, ethanol, 90 °C; (ix) Methyl iodide, NaH, DMF, reflux.

Aminoalkylation of the furan ring of **6a** using 4-aminopyridine and paraformaldehyde (Mannich reaction) was achieved to form **7a** while alkylation of **6a** with benzylamine was performed to give **7b**. Compounds containing the oxadiazole ring **8a**,**b**, 5-[(2-(furan-2-yl)-1*H*-benzo[*d*]imidazol-1-yl)methyl]-1,3,4-oxadiazole-2(3*H*)-thione and the 5-methyl derivative were obtained from the cyclization reaction of the hydrazides **6a**,**b** with carbon disulphide in potassium hydroxide and ethanol. The reaction mechanism involved a nucleophilic attack of the hydrazides **6a**,**b** to the carbon atom of carbon disulfide to form the intermediate **A**. The enol form of **A** (intermediate **B**) underwent ring closure *via* intramolecular nucleophilic attack of the lone pair of electrons of the OH oxygen atom on the carbon of C=S to achieve the compounds **8a**,**b** (Scheme 2) [30].

Then, **8a** reacted with hydrazine hydrate in refluxing ethanol at 90 °C to form compound **10**. The postulated reaction mechanism involved nucleophilic attack of the hydrazine on the α-carbon atom of the oxadiazole ring of **8a** to give the intermediate **C** which undergo ring opening to form **D**. Cyclization of **D** *via* further nucleophilic attack of the hydrazide on the carbon of C=S was performed to form **E** followed by dehydration to achieve the thiol form **F** which was further stabilized to its tautomer thione form **10** (Scheme 3) [31]. S-Alkylation of the thiol form of **8a** with methyl iodide in sodium hydride and DMF at reflux temperature yielded **11**. The reaction of **6a**,**b** with ethyl acetoacetate in potassium hydroxide and ethanol achieved successfully compounds **9a**,**b.** The mechanism of this reaction involves nucleophilic attack of the hydrazides **6a**,**b** to the carbon atom of the C=O of the acetyl group of ethyl acetoacetate to form the target compounds **9a**,**b** [32].

2.2. Bioactivity

2.2.1. Cytotoxicity against human breast cancer cell line MCF-7

Cytotoxicity of the synthesized compounds **3**–**11** was tested using Skehan et al. method [33] in human breast cancer cell line MCF-7. The Cytotoxicity results were compared to that of Tamoxifen. Compound **5a** exhibited higher potency against breast cancer cell line MCF-7 with (IC_{50} = 6.98 μg/ml) lower than that of Tamoxifen whose (IC_{50} = 8.00 μg/ml), while compound **5c** was equipotent to Tamoxifen with (IC_{50} = 8.63 μg/ml). The rest of the compounds were of promising activity against MCF-7 cell line with (IC_{50}: 14.00–22.40 μg/ml) and their order of reactivity was **3b**, **4a**,

Please cite this article in press as: A. Temirak, et al., Part I. Synthesis, biological evaluation and docking studies of new 2-furylbenzimidazoles as antiangiogenic agents, European Journal of Medicinal Chemistry (2014), http://dx.doi.org/10.1016/j.ejmech.2014.01.063

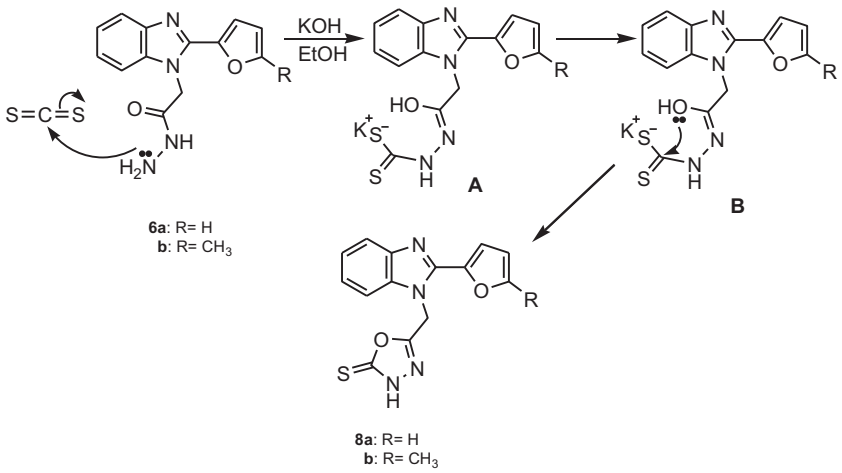

Scheme 2. Synthesis mechanism of compounds **8a**,**b**.

8b, **8a**, **9a**, **4b**, **7b**, **11**, **9b**, **6a**, **10**, **5b**, **3a**, **7a** and **6b** in a descending order as shown in (Table 1).

2.2.2. *In vitro VEGF inhibition in human breast cancer cell line MCF-7*

Angiogenesis is essential for tumor progression because tumor mass cannot grow bigger than 2 mm^3 without the nourishment of blood vessels. Moreover, vascularization is required for the process of extravasation in metastasis [34]. Hence, establishment of chemotherapeutic strategy by blocking angiogenesis attracts much attention in recent years. Besides, alteration of the cellular adaptation to hypoxia is also fundamental in cancer treatment because angiogenesis or other metabolic modifications will be stimulated to maintain tumor cell survival [35]. Vascular endothelial growth factor (VEGF) has been identified as the most important angiogenic factor for tumor progression because it is released by a variety of tumor cells and over expresses in different human cancers. Drugs that can inhibit the production of VEGF or block its receptor signaling show significant inhibition of tumor growth.

This biological *in vitro* study was done using double-antibody sandwich enzyme-linked immunosorbent assay (ELISA) to assay the level of human VEGF in human breast cancer cell line MCF-7 samples as compared to the inhibition for the untreated cells. The screening results (Table 1) showed that most of the tested compounds showed potent inhibition against human VEGF in the tested samples. Nearly six compounds (**3b**, **5a**, **5c**, **6b**, **7a** and **10**) were found to be potent and selective similar to the positive drug, Tamoxifen (98%) with percentage of inhibition values 95, 98, 98, 86, 90, 91% respectively as compared with control untreated cells. From the foregoing result it is clear that these results were consistent with cell cytotoxicity activity, compounds **5a** and **5c** were the most potent compounds against breast cancer cell line MCF-7 and at the same time possess the highest inhibition against the human VEGF activity equal to that of Tamoxifen.

2.2.3. *In vitro cyclooxygenase (COX) inhibition*

Furthermore, we have studied the ability of some of the best active compounds inhibiting human VEGF in breast cancer cell line MCF-7 to inhibit ovine COX-1 and COX-2 using an enzyme immunoassay (EIA) kit. The efficacies of the tested compounds were determined as the concentration causing 50% enzyme inhibition (IC_{50}) (Table 2). All the tested compounds have showed no inhibition of COX-1 with $IC_{50} > 50$ μM. Moreover, a reasonable *in vitro* COX-2 inhibitory activity was observed with compounds **6b**, **7a** and **10** with IC_{50} 0.47, 0.36, 0.4 μM respectively. The selectivity indices (COX-1/COX-2) were calculated and compared with that of the

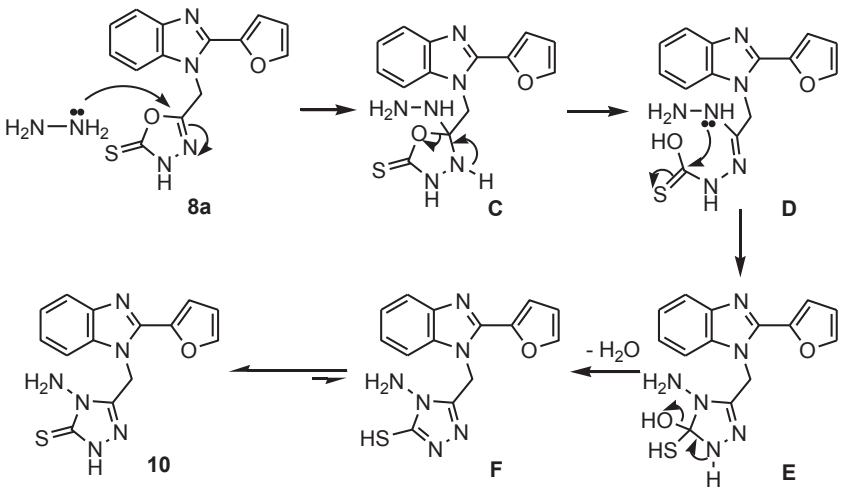

Scheme 3. Synthesis mechanism of compound **10**.

Please cite this article in press as: A. Temirak, et al., Part I. Synthesis, biological evaluation and docking studies of new 2-furylbenzimidazoles as antiangiogenic agents, European Journal of Medicinal Chemistry (2014), http://dx.doi.org/10.1016/j.ejmech.2014.01.063

Table 1
Effect of the synthesized compounds **3**–**11** on the MCF-7 cancer cell line (IC_{50}) and the VEGF level (Pg/ml) in MCF-7 cancer cell line.

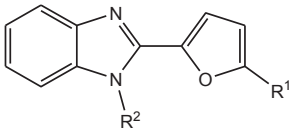

Compound	R^1	R^2	IC_{50} (μg/ml)[a]	VEGF (Pg/ml)[b]	
3a	H	H	21.50	4460.90	(15%)
3b	CH_3	H	14.00	280.24	(95%)
4a	H	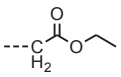	15.20	2000.82	(62%)
4b	CH_3	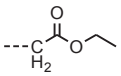	17.80	3760.70	(28%)
5a	H	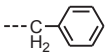	6.98	90.70	(98%)
5b	H	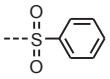	21.20	4514.23	(14%)
5c	CH_3	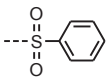	8.63	125.18	(98%)
6a	H	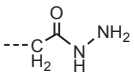	20.20	4010.45	(24%)
6b	CH_3	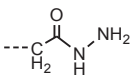	22.40	760.40	(86%)
7a	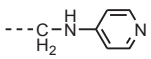	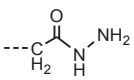	22.00	530.33	(90%)
7b	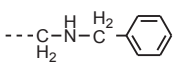	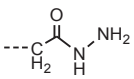	19.30	4280.32	(19%)
8a	H	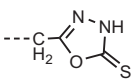	16.90	3112.78	(41%)
8b	CH_3	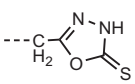	16.60	3200.80	(39%)
9a	H	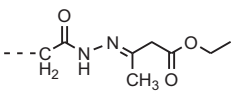	17.00	3265.80	(38%)
9b	CH_3	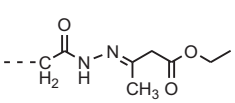	19.60	3978.67	(24%)
10	H	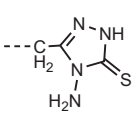	20.50	480.45	(91%)

(*continued on next page*)

Table 1 (*continued*)

Compound	R^1	R^2	IC_{50} (μg/ml)[a]	VEGF (Pg/ml)[b]	
11	H	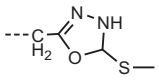	19.30	4420.70	(16%)
DMSO	–	–	–	5250.00	–
Tamoxifen	–	–	8.00	110.75	(98%)

[a] Data were expressed as mean of six independent experiments.
[b] Values between brackets indicated percentage changes as compared with control untreated cells.

standard COX-2 selective inhibitor, Celecoxib whose IC_{50} values on COX-1 and COX-2 were determined to be >50 and 0.28 μM.

The correlation between VEGF inhibition in MCF-7 cancer cell line and selective COX-2 inhibition proves that the antiangiogenic agents targeting VEGFR2 kinase are probably inhibiting COX-2 where there is a significant over expression of COX-2 and VEGF in malignant tumors.

2.3. Molecular docking study

Molecular docking is a frequently used tool in computer-aided structure-based rational drug design. It evaluates how small molecules called (*e.g.* drug candidates) and the target macromolecule (receptor or enzyme) fit together. AutoDock Tools (ADT) is a program package of automated docking tools that is available from http://autodock.scripps.edu/. It is designed to predict how small molecules bind to a target protein of known 3D-structure. Besides generating binding energies in these docking studies, the position of the ligand in the host's binding site can be visualized. It can be useful for developing better drug candidates and also for the understanding the nature of the binding.

In this study, seventeen compounds: **3a**, **3b**, **4a**,**b**, **5a**–**c**, **6a**,**b**, **7a**,**b**, **8a**,**b**, **9a**,**b**, **10** and **11** were docked into the target crystal structure of human VEGFR2 tyrosine kinase domain (PDB code: 3EWH) in complex with a pyridyl-pyrimidine benzimidazole inhibitor (K11).

2.3.1. Evaluation of docking performance and accuracy into VEGFR2 kinase

As cited in (Table 1 enclosed in the supplementary data), the RMSD values for the redocked native PTK inhibitor (K11) was 1.49 Å, where it is found that the docked ligand was superimposed with the originally embedded native ligand. Moreover, it exhibited the lowest binding free energy (ΔG_b) of −13.04 kcal/mol and further three hydrogen bonds with Glu885 (NH) and Cys919 (NH), in addition to non covalent molecular interactions with the residues Lys868 and Phe1047. As cited in literature [36] if the RMSD of the best docked conformation of the native ligand is ≤2.0 Å from the experimental one, the used scoring function is successful. Therefore these results indicated that flexible docking involving AutoDock 4.2 under our experimental parameters seems to be accurate, being of small RMSD values, to be of high resemblance to the biological co-crystallization. Hence, docking result of the natively embedded ligand of VEGFR2 exhibited reasonable well comparable and well correlated to their biological methods.

Table 2
Data of the *in vitro* COX-1/COX-2 enzyme inhibition assay of the designed compounds.

Compound	Cox-1 IC_{50} (μM)[a]	Cox-2 IC_{50} (μM)[a]	SI[b]
6b	>50	0.40	125.0
7a	>50	0.47	106.4
10	>50	0.36	138.9
Celecoxib	>50	0.28	178.6

[a] IC_{50} value is the compound concentration required to produce 50% inhibition of COX-1 or COX-2 for means of two determinations and deviation from the mean is <10% of the mean value.
[b] Selectivity index (SI) (COX-1 IC_{50}/COX-2 IC_{50}).

2.3.2. Docking study of the synthesized compounds

Docking of our new compounds into the VEGFR2 kinase indicated that compounds revealing the lowest binding free energies are **5a**,**c**, **7a**,**b**, **8a** and **9b**. They exhibited (ΔG_b) being: −11.36, −12.56, −11.56, −11.85, −11.53, and −11.38 kcal/mol, respectively with RMSD range of 3.79–7.81 Å. Moreover, they bind into kinase domain through up to two hydrogen bonds, involving their moieties being: imidazole =N, CONH, Ph-NH, Terminal NH which bound to the commonly involved amino acids being: Glu885 (C=O), Asp1046 (NH), Leu840 (C=O), Lys868 (NH), Asn923 (NH), Cys1045 (SH), and Phe1047 (C=O) (as cited in Table 1 in the Supplementary data).

As illustrated in Fig. 3, compound **5a** possess a high potential binding affinity (ΔG_b: −11.66 kcal/mol) into the binding site of the 3D macromolecule (PDB code: 3EWH). Its high affinity is presumably attributed to its hydrogen bond formed between its imidazole C=N moiety and Lys868 (NH) amino acid of the binding site. Compound **10** has a reasonable potential binding affinity (ΔG_b: −10.82 kcal/mol) into the binding site, forming two hydrogen bonds between its terminal NH and SH and Thr916 (OH). In addition, both compounds interact hydrophobically with the surrounding Leu840, Lys868, and Leu889 amino acids.

On applying the flexible docking into VEGFR2 kinase, the high binding affinity was elucidated by lower binding free energy. As shown in Fig. 4 and cited in (as cited in Table 1 enclosed in the Supplementary data), compound **6b** (ΔG_b: −11.47 kcal/mol) has a promising antiproliferative activity through its high PTK binding affinity. Compound **6b** bound into VEGFR2 kinase through one hydrogen bond between its terminal NH and the HN of Lys868 amino acid whereas, compound **3a** revealed high binding energy (ΔG_b: −9.54 kcal/mol) i.e. low binding affinity. These results are highly correlated to the biological results.

In the analysis of docking results, a fair overall correlation exists between the biological results (IC_{50} (μg/ml) against breast cancer cell line) and their corresponding inhibition constants (K_i) predicted by AutoDock into the corresponding VEGFR2 kinase. Where many compound, namely **4b**, **5a**–**c**, **6a**, **8a**,**b**, **9a**, **10** and **11** revealed a reasonable correlation coefficient (R^2) of 0.5513 as represented in Fig. 5(A). Whereas, compounds **3a**, **4b**, **5a**–**c**, **6b**, **7a**, **8b**, **9a**, **10** and **11** revealed significant correlation coefficient (R^2 = 0.4623) between their biological results; %VEGF inhibition against breast cancer cell line MCF-7 and AutoDock binding free energies (ΔG_b) into VEGFR2 kinase, as can be seen in Fig. 5(B) compounds of better binding affinity to VEGFR2 kinase are greatly inhibiting the VEGF level in cancer tissues.

Accordingly, from the aforementioned correlation between the biological activity and molecular docking results, we can conclude

Please cite this article in press as: A. Temirak, et al., Part I. Synthesis, biological evaluation and docking studies of new 2-furylbenzimidazoles as antiangiogenic agents, European Journal of Medicinal Chemistry (2014), http://dx.doi.org/10.1016/j.ejmech.2014.01.063

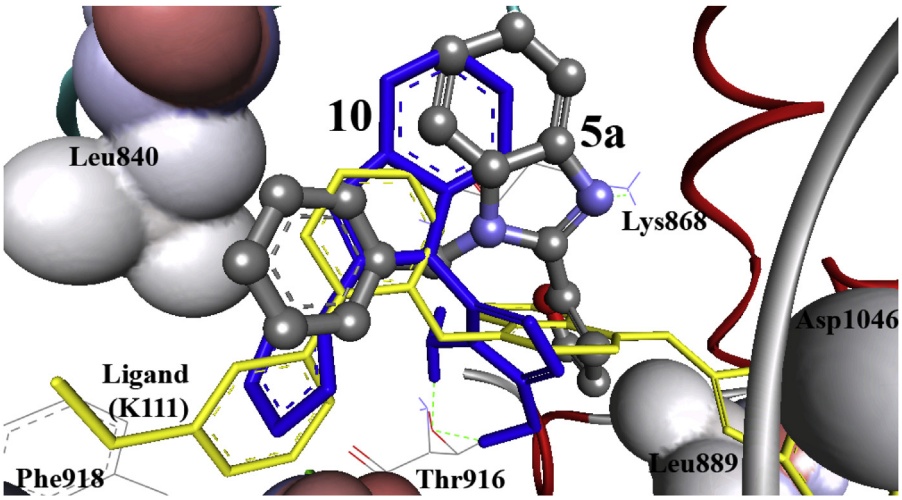

Fig. 3. Comparative docking modes of compounds **5a** (ball and stick, colored by element) and **10** (blue sticks) involving flexible docking into VEGFR2 kinase. Compounds **5a** and **10** exhibited one and two hydrogen bonds, respectively; shown as green dashed lines. They are shown superimposed (RMSD: 3.79 and 3.55 Å) onto the K111 ligand (yellow sticks). PTK is shown as solid backbone ribbon for protein and its and the binding site is shown in solid surface view with labeled amino acids. (For interpretation of the references to color in this figure legend, the reader is referred to the web version of this article.)

that our compounds in this study are showing significant anti-angiogenic inhibition of VEGFR2 kinase.

2.4. Theoretical estimation of partition coefficient

Partition coefficient (log *P*) is a measure of the lipophilicity (octanol/water partition coefficient) of compounds. Acceptable log *P* values are preferable from 1 to 2.5 [37]. We have measured the theoretical log *P* using CS ChemProp in ChemDraw [38]. Most compounds showed acceptable log *P* values as shown in (Table 3).

3. Structure activity relationship

The comparison of the biological activity along with the docking affinities and interactions of the synthesized compounds gave more insight into the structure activity relationship of 2-furyl benzimidazole derivatives as VEGFR2 kinase inhibitors.

The high activity of **5a** and **5c** may be attributed to: (i) the hydrogen bond formed between the C=N of the imidazole ring and Lys868 (NH) amino acid of the binding site; (ii) the role exerted by the aromatic ring at position 1 of benzimidazole moiety causing non covalent molecular interactions (pi–cation interaction); (iii) the CH_2 linker in benzyl group provided flexibility for the aromatic group. The benzyl group in **5a** has more impact on activity than the methylbenzenesulfonyl group in **5c**, due to the bulkiness of the sulfonyl group. The effect of the methyl group on increasing activity was clear, **5c** being more potent than **5b**.

Substitution of the furyl ring by a methyl group at position 5 in the compounds carrying benzyl or methylbenzenesulfonyl in position 1 of the benzimidazole moiety as in **3b**, **5c** and **6b** resulted in better biological activity and binding affinity with the VEGFR2 than **3a**, **5b** and **6a** respectively. This emphasizes the important role of the methyl group in increasing the antiangiogenic activity of the compound by the possible hydrophobic contact with the active site. Additionally, replacing the methyl group at position 5 of the furyl ring with methylaminopyridine group as in **7a** increases the activity, while the substitution with methylbenzylamine as in **7b** demolished the activity of the compound. The pronounced activity of **7a** relative to **7b** indicated the importance of pyridine ring which exhibited H-bonding with the Asp1046 residue on VEGFR2.

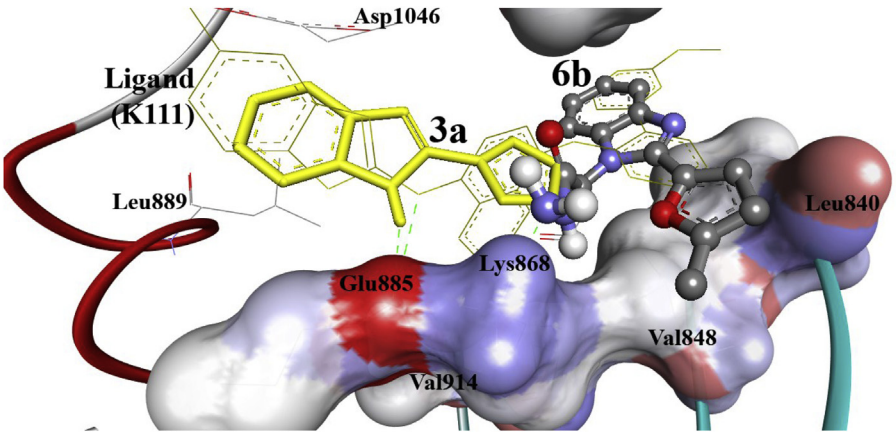

Fig. 4. Comparative docking modes of compounds **3a** (yellow sticks) and **6b** (ball and stick, colored by element), involving flexible docking into VEGFR2 kinase. They exhibited one hydrogen bond for each; shown as green dashed lines with Glu885 and Lys868, respectively. Compound **6b** is shown deeply embedded within the groove of the binding site. PTK is shown as solid backbone ribbon for protein and its and the binding site is shown in solid surface view with labeled amino acids. (For interpretation of the references to color in this figure legend, the reader is referred to the web version of this article.)

Please cite this article in press as: A. Temirak, et al., Part I. Synthesis, biological evaluation and docking studies of new 2-furylbenzimidazoles as antiangiogenic agents, European Journal of Medicinal Chemistry (2014), http://dx.doi.org/10.1016/j.ejmech.2014.01.063

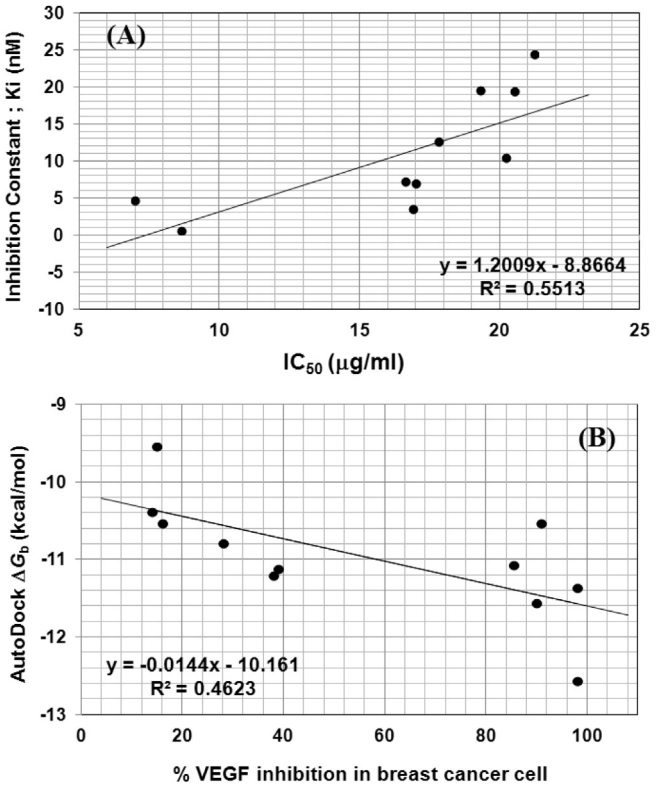

Fig. 5. (**A**) The overall correlation between IC_{50} against breast cancer cell line and the inhibition constants (K_i) for compounds **4b**, **5a**–**c**, **6a**, **8a**,**b**, **9a**, **10**, and **11** into VEGFR2 kinase. (**B**) The correlation between %VEGF inhibition in breast cancer cell line MCF-7 and the binding free energies (ΔG_b) for compounds **3a**, **4b**, **5a**–**c**, **6b**, **7a**, **8b**, **9a**, **10**, and **11** into VEGFR2 kinase.

Changing the substitution at position 1 from oxadiazole ring in **8a** to triazole ring with terminal NH_2 group in **10** increased the activity, due to the H-bonding of the electron donating NH_2 group with Thr916. The furyl ring in the 2-furylbenzimdazole derivatives could form noncovalent molecular hydrophobic interactions with the Lys868 residue in VEGFR2 kinase active site quite similar to that made by the naphthalene ring in the native ligand (K11). This could explain the closefitting of the 2-furylbenzimdazoles to the VEGFR2 kinase.

In conclusion, optimizing the activity of 2-furylbenzimidazole derivatives as anti VEGFR2 kinase could be through the following substitutions:

a) By a methyl group at position 5 of the furan ring as in **3b** and **5c.**
b) By an aromatic ring with electronegative nitrogen as pyridine linked to position 5 of the furan ring through NH–CH_2 linker as in **7a.**
c) By an aromatic group at position 1 of the benzimidazole moiety, linked by a flexible linker, as in compound **5a.**
d) By a triazole ring, carrying the electron donating nitrogen atoms, at position 1 of benzimidazole as in **10.**

Table 3
Theoretical partition coefficient (log *P*) of the 2-furylbenzimidazole derivatives **3**–**11**.

Compound	Theoretical log *P*	Compound	Theoretical log *P*	Compound	Theoretical log *P*
3a	1.48	**5c**	3.26	**8b**	2.15
3b	1.82	**6a**	0.08	**9a**	0.84
4a	1.58	**6b**	0.42	**9b**	1.18
4b	1.92	**7a**	0.03	**10**	2.08
5a	3.45	**7b**	1.58	**11**	2.65
5b	2.93	**8a**	1.82		

4. Conclusion

Our main goal throughout this manuscript was the synthesis of new (2-furyl)-1H-benzimidazole derivatives as antiangiogenic agents working *via* inhibiting VEGF-VEGFR2 complex formation, thus suppressing proliferation and survival of endothelial cells and consequently preventing cancer progression.

Some analogues for the drug candidates NP-184 **5** and PJ-8 **6** have been synthesized showing potential inhibition of VEGF induced angiogenesis. Scheme 1 outlined the synthetic steps of the target compounds **3**–**11** and the existence of these compounds was verified using spectral and microanalyses data.

The bioactivity of the compounds **3**–**11** showed that 6 compounds (**3b**, **5a**, **5c**, **6b**, **7a** and **10**) have shown promising cytotoxic activity against breast cancer cell line MCF-7 with (IC_{50}: 6.98–22.40 μg/ml) and potential inhibition of human VEGF in MCF-7 cancer cell line with percentages of inhibition (86–98%) in comparison to the positive drug, Tamoxifen (IC_{50}: 8.00 μg/ml, % inhibition = 98%) as compared with control untreated cells. Moreover, compounds **6b**, **7a** and **10** expressed selective inhibition of COX-2 enzyme in comparison to COX-1 enzyme with selectivity indices quite similar to that of Celecoxcib.

Furthermore, molecular docking studies were done using AutoDock 4.2 in order to understand the binding modes and inhibitory effect of the synthesized compounds **3**–**11** against the receptor tyrosine kinase VEGFR2, Compounds **5a**,**c**, **7a**,**b**, **8a**, and **9b** showed promising binding interactions with the receptor. Considerable correlation exists between the biological activity results (IC_{50} and %VEGF inhibition) against MCF-7 cell line and the molecular docking results (K_i and ΔG_b) with correlation coefficient (R^2) of 0.5513 and 0.4623 respectively. Synthesized analogues of 2-(2-furyl)-1H-benzimidazole have shown potential inhibition of VEGFR2 kinase which may argument their advantage as promising antiangiogenic agents.

4.1. Physical measurements

Microanalyses and spectral data of the compounds were performed in the Micro analytical labs, National Research Centre and Micro analytical Laboratory Center, Faculty of Science, Cairo University, Cairo, Egypt. The IR spectra (4000–400 cm^{-1}) were recorded using KBr pellets in a Jasco FT/IR 300E Fourier transform infrared spectrophotometer on a Perkin Elmer FT-IR 1650 (spectrophotometer). The melting points were determined on a Stuart SMP30 Melting Point Apparatus and are uncorrected. The H^1 and C^{13} NMR spectra were recorded using Joel ECA 500 MHz NMR spectrophotometers using DMSO-d_6 as a solvent. Chemical shifts are reported in parts per million (ppm) from the tetramethylsilane resonance in the indicated solvent. Coupling constants are reported in Hertz (Hz); spectral splitting partners are designed as follow: singlet (s); doublet (d); triplet (t); multiplet (m). The mass spectra were carried out using Finnigan mat SSQ 7000 (Thermo. Inst. Sys. Inc., USA) spectroscopy at 70 ev. Reaction progress was monitored using thin layer chromatography (TLC) analysis on Silica Gel 60 F254 plate (Merck).

4.1.1. General procedure for the preparation of compounds (*3a,b*) [29]

1,2-Phenylenediamine **1** (10.8 g, 0.1 mol) and (0.1 mol) of furfural **2a** or 5-methylfurfural **2b** were mixed in DMF (10 ml), then *p*-toluenesulfonic acid (3.4 g, 0.02 mol) was added, and the solution

was heated and stirred at 100 °C for 2 h. When the reaction was completed, the reaction mixture was cooled and added dropwise with vigorous stirring onto a mixture of anhydrous Na_2CO_3 (10.6 g, 0.1 mol) and distilled H_2O (20 ml). The product was collected by filtration, washed with H_2O and dried.

4.1.2. 2-(Furan-2-yl)-1H-benzo[d]imidazole (**3a**)

Yield = 85% (15.63 g). M.p.: 285–287 °C. TLC R_f = 0.57 (petroleum ether/ethyl acetate, 2:1). ^{1}H NMR (DMSO-d_6) δ: 6.69 (dd, J = 3 Hz, 1H, H_4 2-furyl), 7.15 (dd, J = 3 Hz, 1H, H_3 2-furyl), 7.16–7.17 (m, 2H, H_5 + H_6 benzimidazole), 7.49–7.51 (m, 2H, H_4 + H_7 benzimidazole), 7.90 (dd, J = 3 Hz, 1H, H_5 2-furyl), 13.00 (s, 1H, NH, D_2O exchangeable). IR (cm^{-1}): 3435 (NH), 1629 (C=N). MS: m/z 185, 14% (M^++1); m/z 184, 100% (M^+); m/z 183, 21% (M^+−1); m/z 156, 25% (M^+−CO). Anal. Calcd for $C_{11}H_8N_2O$ (184.06): C, 71.73; H, 4.38; N, 15.21. Found C, 71.65; H, 4.41; N, 15.25.

4.1.3. 2-(5-Methylfuran-2-yl)-1H-benzo[d]imidazole (**3b**)

Yield = 80% (15.92 g). M.p.: 275–277 °C. TLC R_f = 0.49 (petroleum ether/ethyl acetate, 2:1). ^{1}H NMR (DMSO-d_6) δ: 2.36 (s, 3H, CH_3), 6.31 (d, J = 3 Hz, 1H, H_4 2-furyl), 7.05 (d, J = 3 Hz, 1H, H_3 2-furyl), 7.13–7.15 (m, 2H, H_5 + H_6 benzimidazole), 7.49–7.50 (m, 2H, H_4 + H_7 benzimidazole), 12.00 (s,1H, NH, D_2O exchangeable). IR (cm^{-1}): 3446 (NH), 1632 (C=N). MS: m/z 199, 5% (M^++1); m/z 198, 100% (M^+); m/z 183, 30% (M^+−CH_3); m/z 169, 33%; m/z 155, 24%. Anal. Calcd for $C_{12}H_{10}N_2O$ (198.08): C, 72.71; H, 5.08; N, 14.13. Found C, 72.77; H, 5.02; N, 14.16.

4.1.4. General procedure for the preparation of compounds (**4a**,**b**)

To a well stirred solution of benzimidazoles (**3a** or **3b**) (0.01 mol) and anhydrous K_2CO_3 (1.06 g, 0.01 mol) in dry acetone, ethyl 2-bromoacetate (1.1 ml, 0.01 mol) was added dropwise. The reaction mixture was stirred for 3 h at room temperature. The reaction mixture was poured onto cold water and the precipitate was filtered, dried and recrystallized from ethanol.

4.1.5. Ethyl 2-(2-(furan-2-yl)-1H-benzo[d]imidazol-1-yl)acetate (**4a**)

Yield = 90% (2.43 g). M.p.: 150–152 °C. TLC R_f = 0.65 (petroleum ether/ethyl acetate, 2:1). ^{1}H NMR (DMSO-d_6) δ: 1.15 (t, J = 2.3 Hz, 3H, CH_2CH_3), 4.12 (q, J = 2.3 Hz, 2H, CH_2CH_3), 5.43 (s, 2H, CH_2), 6.70 (dd, J = 3 Hz, 1H, H_4 2-furyl), 7.17 (dd, J = 3 Hz, 1H, H_3 2-furyl), 7.23–7.24 (m, 2H, H_5 + H_6 benzimidazole), 7.62–7.63 (m, 2H, H_4 + H_7 benzimidazole), 7.90 (dd, J = 3 Hz, 1H, H_5 2-furyl). IR (cm^{-1}): 1742 (C=O), 1610 (C=N). MS: m/z 271, 14% (M^++1); m/z 270, 84% (M^+); m/z 269, 3%; m/z 197, 100%, (M^+−$COOC_2H_5$). Anal. Calcd for $C_{15}H_{14}N_2O_3$ (270.10): C, 66.66; H, 5.22; N, 10.36. Found C, 66.58; H, 5.24; N, 10.45.

4.1.6. Ethyl 2-(2-(5-methylfuran-2-yl)-1H-benzo[d]imidazol-1-yl) acetate (**4b**)

Yield = 85% (2.41 g). M.p.: 88–90 °C. TLC R_f = 0.60 (petroleum ether/ethyl acetate, 2:1). ^{1}H NMR (DMSO-d_6) δ: 1.17 (t, J = 2.3 Hz, 3H, CH_2CH_3), 2.33 (s, 3H, CH_3), 4.14 (q, J = 2.3 Hz, 2H, CH_2CH_3), 5.05 (s, 2H, CH_2), 6.33 (d, J = 3 Hz, 1H, H_4 2-furyl), 7.05 (d, J = 3 Hz, 1H, H_3 2-furyl), 7.21–7.23 (m, 2H, H_5 + H_6 benzimidazole), 7.59–7.61 (m, 2H, H_4 + H_7 benzimidazole). ^{13}C NMR (500 MHZ, DMSO-d_6): 13.83, 14.59, 47.00, 61.75, 108.99, 110.69, 113.96, 119.28, 122.96, 123.14, 136.36, 142.90, 143.98, 144.52, 154.50, 169.07. IR (cm^{-1}): 1748 (C=O), 1616 (C=N). MS: m/z 285, 99% (M^++1); m/z 284, 93% (M^+); m/z 256, 13% (M^+−C_2H_5); m/z 211, 81%; m/z 183, 25% (M^+−$CH_2COOC_2H_5$−CH_3). Anal. Calcd for $C_{16}H_{16}N_2O_3$ (284.12): C, 67.59; H, 5.67; N, 9.85. Found C, 67.50; H, 5.60; N, 9.89.

4.1.7. General procedure for the preparation of compounds (**5a**–**c**)

To a well stirred solution of benzimidazoles (**3a** or **3b**) (0.01 mol) and anhydrous K_2CO_3 (1.06 g, 0.01 mol) in dry acetone, benzyl chloride and benzenesulphonyl chloride (0.01 mol) were added dropwise. The reaction mixture was stirred for 3 h at room temperature. Excess acetone was evaporated under reduced pressure and the reaction mixture was poured onto cold water and the precipitate obtained was filtered, dried and recrystallized from ethanol.

4.1.8. 1-Benzyl-2-(furan-2-yl)-1H-benzo[d]imidazole (**5a**)

Yield = 85% (2.30 g). M.p.: 255–257 °C. TLC R_f = 0.67 (petroleum ether/ethyl acetate, 2:1). ^{1}H NMR (DMSO-d_6) δ: 5.78 (s, 2H, CH_2), 6.70 (dd, J = 3 Hz, 1H, H_4 2-furyl), 7.06–7.08 (m, 2H, H_5 + H_6 benzimidazole), 7.14 (dd, J = 3 Hz, 1H, H_3 2-furyl), 7.20-7.30 (m, 5H, $H_{2'}$–$H_{6'}$ phenyl), 7.57–7.60 (m, 2H, H_4 + H_7 benzimidazole), 7.93 (dd, J = 3 Hz, 1H, H_5 2-furyl). ^{13}C NMR (500 MHZ, DMSO-d_6): 48.26, 111.66, 112.92, 114.71, 118.87, 122.64, 123.84, 124.08, 126.91, 128.11, 129.27, 132.21, 135.65, 137.14, 141.19, 143.61, 144.14, 146.22. IR (cm^{-1}): 1607 (C=N). MS: m/z 375, 7% (M^++1); m/z 374, 39% (M^+); m/z 373, 10% (M^+−1); m/z 197, 93%. Anal. Calcd for $C_{18}H_{14}N_2O$ (274.11): C, 78.85; H, 5.19; N, 10.11. Found C, 78.83; H, 5.12; N, 10.20.

4.1.9. 1-(Benzenesulfonyl)-2-(furan-2-yl)-1H-1,3-benzodiazole (**5b**)

Yield = 80% (2.60 g). M.p.: 112–114 °C. TLC R_f = 0.62 (petroleum ether/ethyl acetate, 2:1). ^{1}H NMR (DMSO-d_6) δ: 6.70 (dd, J = 3 Hz, 1H, H_4 2-furyl), 7.18 (dd, J = 3 Hz, 1H, H_3 2-furyl), 7.23–7.26 (m, 2H, H_5 + H_6 benzimidazole), 7.56–7.60 (m, 2H, H_4 + H_7 benzimidazole), 7.70–7.90 (m, 5H, $H_{2'}$ – $H_{6'}$ phenyl), 8.06 (dd, J = 3 Hz, 1H, H_5 2-furyl). IR (cm^{-1}): 1615 (C=N), 1368 and 1160 (S=O). MS: m/z 325, 6% (M^++1); m/z 324, 26% (M^+); m/z 323, 13% (M^+−1); m/z 184, 33%. Anal. Calcd for $C_{17}H_{12}N_2O_3S$ (324.06): C, 62.97; H, 3.78; N, 8.58; S, 9.82. Found C, 62.93; H, 3.72; N, 8.65; S, 9.87.

4.1.10. 1-(Benzenesulfonyl)-2-(5-methylfuran-2-yl)-1H-1,3-benzodiazole (**5c**)

Yield = 78% (2.63 g). M.p.: 166–168 °C. TLC R_f = 0.65 (petroleum ether/ethyl acetate, 2:1). ^{1}H NMR (DMSO-d_6) δ: 2.36 (s, 3H, CH_3), 6.21 (d, J = 3.05 Hz, 1H, H_4 2-furyl), 7.27 (d, J = 3.05 Hz, 1H, H_3 2-furyl), 7.37–7.39 (m, 2H, H_5 + H_6 benzimidazole), 7.55–7.60 (m, 2H, H_4 benzimidazole), 7.72–7.74 (m, 5H, $H_{2'}$ + $H_{3'}$ + $H_{4'}$ + $H_{5'}$ + $H_{6'}$ phenyl protons), 8.16–8.18 (m, 2H, H_7 benzimidazole). ^{13}C NMR (500 MHZ, DMSO-d_6): 13.90, 108.97, 110.74, 114.42, 114.99, 117.65, 120.77, 126.05, 127.28, 128.25, 129.14, 130.47, 135.76, 137.90, 141.21, 142.39, 144.05, 155.87. IR(cm^{-1}): 1610 (C=N), 1370 and 1154 (S=O). MS: m/z 340, 5% (M^++2); m/z 338, 80% (M^+); m/z 197, 100%; m/z 183, 5%. Anal. Calcd for $C_{18}H_{14}N_2O_3S$ (338.07): C, 63.89; H, 4.17; N, 8.28; S, 9.48. Found C, 63.80; H, 4.19; N, 8.34; S, 9.49.

4.1.11. General procedure for the preparation of compounds (**6a**,**b**)

To a solution of benzimidazoles (**4a** or **4b**) (0.01 mol) in methanol (15 ml), hydrazine hydrate (0.02 mol) was added dropwise and the reaction mixture was refluxed for 4 h. The reaction mixture was cooled and the excess solvent was evaporated using reduced pressure. The product separated was filtered, washed with small portions of cold ethanol and cold water repeatedly and dried. The product was purified by recrystallization from ethanol.

4.1.12. 2-(2-(Furan-2-yl)-1H-benzo[d]imidazol-1-yl) acetohydrazide (**6a**)

Yield = 88% (2.25 g). M.p.: 240–242 °C. TLC R_f = 0.70 (petroleum ether/ethyl acetate, 1:1). ^{1}H NMR (DMSO-d_6) δ: 4.31 (s, 2H, NH_2, D_2O exchangeable), 5.10 (s, 2H, CH_2), 6.70 (dd, J = 3 Hz, 1H, H_4 2-furyl), 7.14 (dd, J = 3 Hz, 1H, H_3 2-furyl), 7.22–7.23 (m, 2H, H_5 + H_6 benzimidazole), 7.49 (m, 1H, H_4 benzimidazole), 7.62 (m,

Please cite this article in press as: A. Temirak, et al., Part I. Synthesis, biological evaluation and docking studies of new 2-furylbenzimidazoles as antiangiogenic agents, European Journal of Medicinal Chemistry (2014), http://dx.doi.org/10.1016/j.ejmech.2014.01.063

1H, H_7 benzimidazole), 7.90 (dd, $J = 3$ Hz, 1H, H_5 2-furyl), 11.00 (s, 1H, NH, D_2O exchangeable). IR (cm^{-1}): 3325 and 3245 (NH and NH_2), 1650 (C=O), 1616 (C=N). MS: *m/z* 271, 5% (M^++1); *m/z* 270, 100% (M^+); *m/z* 253, 7% (M^+-NH_2); *m/z* 211, 81% ($M^+-CONHNH_2$); *m/z* 198, 30% ($M^+-CH_2CONHNH_2$). Anal. Calcd for $C_{13}H_{12}N_4O_2$ (256.10): C, 60.93; H, 4.72; N, 21.86. Found C, 60.98; H, 4.77; N, 21.84.

4.1.13. 2-(2-(5-Methylfuran-2-yl)-1H-benzo[d]imidazol-1-yl) acetohydrazide (**6b**)

Yield = 90% (2.43 g). M.p.: 246–248 °C. TLC $R_f = 0.57$ (petroleum ether/ethyl acetate, 1:1). ^1H NMR (DMSO-d_6) δ: 2.35 (s, 3H, CH_3), 4.30 (s, 2H, D_2O exchangeable), 5.00 (s, 2H, CH_2), 6.30 (d, $J = 3$ Hz, 1H, H_4 2-furyl), 7.00 (d, $J = 3$ Hz, 1H, H_3 2-furyl), 7.20–7.25 (m, 2H, $H_5 + H_6$ benzimidazole), 7.57–7.60 (m, 2H, $H_4 + H_7$ benzimidazole). IR (cm^{-1}): 3348 and 3252 (NH and NH_2), 1660 (C=O), 1612 (C=N). MS: *m/z* 271, 4% (M^++1); *m/z* 270, 100% (M^+); *m/z* 253, 17% (M^+-NH_2); *m/z* 211, 65% ($M^+-CONHNH_2$); *m/z* 198, 42% ($M^+-CH_2CONHNH_2$). Anal. Calcd for $C_{14}H_{14}N_4O_2$ (270.11): C, 62.21; H, 5.22; N, 20.73. Found C, 62.27; H, 5.27; N, 20.79.

4.1.14. General procedure for the preparation of compounds (**7a**,**b**)

To a solution of the acid hydrazide (**6a** or **6b**) (5 mmol) in methanol (20 ml) was stirred at room temperature with para-formaldehyde (0.01 g), conc. hydrochloric acid (1 ml) and primary amine (5 mmol) namely: 4-amino pyridine and benzylamine for 1 h. The reaction mixture was refluxed for 2 h, filtered while hot, and the filtrate was concentrated to one-third of its original volume. The residual liquid was cooled for 24 h. The product that separated out was washed and recrystallized from methanol.

4.1.15. 2-(2-(5-((Pyridin-4-ylamino)methyl)furan-2-yl)-1H-benzo [d]imidazol-1-yl)acetohydrazide (**7a**)

Yield = 72% (1.30 g). M.p.: >300 °C. TLC $R_f = 0.67$ (petroleum ether/ethyl acetate/ethanol, 1:1:1). ^1H NMR (DMSO-d_6) δ: 4.64 (s, 2H, CH_2 2-furyl), 5.70 (s, 2H, CH_2), 5.90 (NH_2, D_2O exchangeable), 6.67 (d, $J = 3$ Hz, 1H, H_4 2-furyl), 7.05 (d, $J = 3$ Hz, 1H, H_3 2-furyl), 7.14–7.15 (m, 2H, $H_5 + H_6$ benzimidazole), 7.40–7.50 (m, 2H, $H_4 + H_7$ benzimidazole), 7.85–7.91 (m, 4H, pyridyl). IR (cm^{-1}): 3390 and 3173 (NH and NH_2), 1680 (C=O), 1610 (C=N). MS: *m/z* 362, 45% (M^+); *m/z* 332, 56% ($M^+-N_2H_3$); *m/z* 197, 95%; *m/z* 184, 48%. Anal. Calcd for $C_{19}H_{18}N_6O_2$ (362.15): C, 62.97; H, 5.01; N, 23.19. Found C, 63.05; H, 5.10; N, 23.24.

4.1.16. 2-(2-(5-((Benzylamino)methyl)furan-2-yl)-1H-benzo[d] imidazol-1-yl)acetohydrazide (**7b**)

Yield = 78% (1.46 g). M.p.: >300 °C. TLC $R_f = 0.70$ (petroleum ether/ethyl acetate/ethanol, 1:1:1). ^1H NMR (DMSO-d_6) δ: 3.58 (s, 2H, CH_2 benzylic), 3.97 (s, 2H, CH_2 2-furyl), 5.70 (s, 2H, CH_2), 6.67 (d, $J = 3$ Hz, 1H, H_4 2-furyl), 7.20 (d, $J = 3$ Hz, 1H, H_3 2-furyl), 7.22–7.25 (m, 2H, $H_5 + H_6$ benzimidazole), 7.36–7.38 (m, 1H, $H_{4'}$ phenyl), 7.40–7.42 (m, 2H, $H_{3'} + H_{5'}$ phenyl), 7.45–7.47 (m, 2H, $H_4 + H_7$ benzimidazole), 7.74–7.76 (m, 2H, $H_{2'} + H_{6'}$ phenyl), 10.80 (s, 1H, NH, D_2O exchangeable), 11.30 (s, 1H, NH, D_2O exchangeable). IR (cm^{-1}): 3408 and 3185 (NH and NH_2), 1685 (C=O), 1612 (C=N). MS: *m/z* 375, 36% (M^+); *m/z* 344, 68% ($M^+-N_2H_3$); *m/z* 197, 100%; *m/z* 184, 60%. Anal. Calcd for $C_{21}H_{21}N_5O_2$ (375.17): C, 67.18; H, 5.64; N, 18.65. Found C, 67.24; H, 5.67; N, 18.68.

4.1.17. General procedure for the preparation of compounds (**8a**,**b**)

Carbon disulfide (0.5 ml) was added dropwise to an ice cooled solution of KOH (0.2 g) in ethanol (10 ml) containing the acid hydrazide (**6a** or **6b**) (5 mmol). The reaction mixture was stirred at room temperature 2 h. After dilution with ethanol, the solid obtained was washed twice with ether. To the solid obtained (0.2 g), 10% KOH (10 ml) was added, then the reaction mixture was refluxed for 10 h, cooled, acidified with conc. HCl. The resulting solid was filtered, washed with water, dried and crystallized from DMF.

4.1.18. 5-((2-(Furan-2-yl)-1H-benzo[d]imidazol-1-yl)methyl)-1,3,4-oxadiazole-2(3H)-thione (**8a**)

Yield = 80% (1.20 g). M.p.: 260–262 °C. TLC $R_f = 0.68$ (petroleum ether/ethyl acetate, 1:1). ^1H NMR (DMSO-d_6) δ: 5.90 (s, 2H, CH_2), 6.74 (dd, $J = 3$ Hz, 1H, H_4 2-furyl), 7.26 (dd, $J = 3$ Hz, 1H, H_3 2-furyl), 7.28–7.30 (m, 2H, $H_5 + H_6$ benzimidazole), 7.65–7.67 (m, 2H, $H_4 + H_7$ benzimidazole), 7.95 (dd, $J = 3$ Hz, 1H, H_5 2-furyl), 11.00 (s, 1H, NH, D_2O exchangeable). ^{13}C NMR (500 MHZ, DMSO-d_6): 46.50, 111.10, 112.83, 113.77, 119.71, 123.61, 123.92, 135.85, 142.78, 144.05, 144.74, 145.94, 159.85, 178.51. IR (cm^{-1}): 3425 (NH), 1612 (C=N), 1120 (C=S). MS: *m/z* 300, 2% (M^++2); *m/z* 299, 18% (M^++1); *m/z* 298, 100% (M^+); *m/z* 297, 21% (M^+-1). Anal. Calcd for $C_{14}H_{10}N_4O_2S$ (298.05): C, 56.37; H, 3.38; N, 18.78; S, 10.75. Found C, 56.32; H, 3.46; N, 18.85; S, 10.78.

4.1.19. 5-((2-(5-Methylfuran-2-yl)-1H-benzo[d]imidazol-1-yl) methyl)-1,3,4-oxadiazole-2(3H)-thione (**8b**)

Yield = 84% (1.31 g). M.p.: 265–267 °C. TLC $R_f = 0.68$ (petroleum ether/ethyl acetate, 1:1). ^1H NMR (DMSO-d_6) δ: 2.34 (s, 3H, CH_3), 5.90 (s, 2H, CH_2), 6.34 (d, $J = 3.05$ Hz, 1H, H_4 2-furyl), 7.05 (d, $J = 3.05$ Hz, 1H, H_3 2-furyl), 7.24–7.29 (m, 2H, $H_5 + H_6$ benzimidazole), 7.62–7.67 (m, 2H, $H_4 + H_7$ benzimidazole). IR (cm^{-1}): 3428 (NH), 1611 (C=N), 1122 (C=S). MS: *m/z* 314, 3% (M^++2); *m/z* 312, 26% (M^+); *m/z* 253, 44%; *m/z* 237, 93%; *m/z* 211, 44%. Anal. Calcd for $C_{15}H_{12}N_4O_2S$ (312.10): C, 57.68; H, 3.87; N, 17.94; S, 10.27. Found C, 57.74; H, 3.83; N, 17.99; S, 10.28.

4.1.20. General procedure for the preparation of compounds (**9a**,**b**)

A mixture of hydrazide (**6a** or **6b**) (5 mmol) and ethyl acetoacetate (2 ml) was refluxed for 5 h. The reaction mixture was diluted with petroleum ether (60–80) and the resulting solid was filtered, washed with water, dried and crystallized from acetic acid and the reaction mixture was then cooled, acidified with conc. HCl. The resulting solid was filtered, washed with water, dried and crystallized from acetic acid.

4.1.21. Ethyl 3-(2-(2-(furan-2-yl)-1H-benzo[d]imidazol-1-yl) acetoylimino)butanoate (**9a**)

Yield = 70% (1.30 g). M.p.: 145–147 °C. TLC $R_f = 0.60$ (petroleum ether/ethyl acetate, 1:1). ^1H NMR (DMSO-d_6) δ: 1.17 (t, 3H, CH_2CH_3), 1.90 (t, 3H, CH_3), 4.10 (s, 2H, CH_2CH_3), 5.30 (s, 2H, $CH_2COOC_2H_5$), 5.54 (s, 2H, CH_2 "benzimidazole attached"), 6.69 (dd, $J = 3$ Hz, 1H, H_4 2-furyl), 7.10 (dd, $J = 3$ Hz, 1H, H_3 2-furyl), 7.14–7.28 (m, 2H, $H_5 + H_6$ benzimidazole), 7.53–7.624 (m, 2H, $H_4 + H_7$ benzimidazole), 7.90 (dd, $J = 3$ Hz, 1H, H_5 2-furyl), 11.0 (s, 1H, NH, D_2O exchangeable). IR (cm^{-1}): 3423 (NH), 1733 (C=O), 1685 (C=O), 1615 (C=N). MS: *m/z* 324, 24% ($M^+-OC_2H_5$); *m/z* 323, 14% ($M^+-OC_2H_5-1$); *m/z* 296, 29% ($M^+-COOC_2H_5$); *m/z* 184, 32% (2-furylbenzimidazole). Anal. Calcd for $C_{19}H_{20}N_4O_2$ (368.15): C, 61.95; H, 5.47; N, 15.21. Found C, 62.07; H, 5.56; N, 15.26.

4.1.22. Ethyl 3-(2-(2-(5-methylfuran-2-yl)-1H-benzo[d]imidazol-1-yl)acetoylimino)butanoate (**9b**)

Yield = 82% (1.56 g). M.p.: 160–162 °C. TLC $R_f = 0.65$ (petroleum ether/ethyl acetate, 1:1). ^1H NMR (DMSO-d_6) δ: 1.16 (t, 3H, CH_2CH_3), 1.90 (t, 3H, CH_3), 2.30 (t, 3H, CH_3 2-furyl), 4.11 (s, 2H, CH_2CH_3), 5.30 (s, 2H, $CH_2COOC_2H_5$), 5.57 (s, 2H, CH_2 "benzimidazole attached"), 6.30 (dd, $J = 3$ Hz, 1H, H_4 2-furyl), 6.95 (d, $J = 3$ Hz, 1H, H_3 2-furyl), 7.15–7.27 (m, 2H, $H_5 + H_6$ benzimidazole), 7.53–7.61 (m, 2H, $H_4 + H_7$ benzimidazole), 10.80 (s, 1H, NH, D_2O exchangeable). IR (cm^{-1}): 3420 (NH), 1730 (C=O), 1685 (C=O), 1617 (C=N). MS: *m/z*

Please cite this article in press as: A. Temirak, et al., Part I. Synthesis, biological evaluation and docking studies of new 2-furylbenzimidazoles as antiangiogenic agents, European Journal of Medicinal Chemistry (2014), http://dx.doi.org/10.1016/j.ejmech.2014.01.063

336, 70% ($M^+-OC_2H_5$); *m/z* 335, 24% ($M^+-OC_2H_5-1$); *m/z* 242, 59%; *m/z* 210, 63%. Anal. Calcd for $C_{20}H_{22}N_4O_2$ (382.16): C, 61.95; H, 5.47; N, 15.21. Found C, 62.03; H, 5.52; N, 15.27.

4.1.23. 5-((2-(Furan-2-yl)-1H-benzo[d]imidazol-1-yl) methyl)-4-amino-4H-1,2,4-triazole-3-thiol (**10**)

To a solution of compound **8a** (2 mmol) in methanol (5 ml), hydrazine hydrate (2 mmol) was added and the reaction mixture was refluxed for 4 h, cooled and the excess solvent was evaporated using reduced pressure. The product separated was filtered, washed and dried. The product was purified by recrystallizion from ethanol. Yield = 85% (0.53 g). M.p.: 277–279 °C. TLC R_f = 0.74 (petroleum ether/ethyl acetate, 1:3). ^{1}H NMR (DMSO-d_6) δ: 5.80 (s, 2H, CH_2), 6.68 (dd, J = 3 Hz, 1H, H_4 2-furyl), 7.18 (dd, J = 3 Hz, 1H, H_3 2-furyl), 7.23–7.25 (m, 2H, $H_5 + H_6$ benzimidazole), 7.64–7.67 (m, 2H, $H_4 + H_7$ benzimidazole), 7.90 (dd, J = 3 Hz, 1H, H_5 2-furyl), 13.50 (s, 2H, NH_2, D_2O exchangeable). ^{13}C NMR (500 MHZ, DMSO-d_6): 48.60, 110.05, 112.69, 113.49, 119.51, 123.35, 123.68, 130.09, 142.68, 144.35, 144.97, 145.71, 149.08, 167.45. IR (cm^{-1}): 3423 and 3285 (NH, NH_2), 1690 (C=O), 1615 (C=N). MS: *m/z* 314, 3% (M^++2); *m/z* 312, 49% (M^+); *m/z* 297, 25% (M^+-NH_2); *m/z* 184, 100%. Anal. Calcd for $C_{14}H_{12}N_6O_2S$ (312.08): C, 53.83; H, 3.87; N, 26.91; S, 10.27. Found C, 53.89; H, 3.94; N, 26.95; S, 10.29.

4.1.24. 2-(Furan-2-yl)-1-(5-(methylthio)-1,3,4-oxadiazol-2-yl)-1H-benzo[d]imidazole (**11**)

To a solution of compound **8a** (2 mmol) in dry DMF, NaH (0.10 g) was stirred at room temperature for 0.5 h. Then, methyl iodide (2 mmol) was added and the reaction mixture was refluxed for 4 h. After cooling the reaction mixture, it was poured onto cold water and the precipitated product was filtered, washed and recrysallized from ethanol. Yield = 74% (0.47 g). M.p.: 278–281 °C. TLC R_f = 0.58 (petroleum ether/ethyl acetate, 1:3). ^{1}H NMR (DMSO-d_6) δ: 2.60 (s, 3H, CH_3), 6.00 (s, 2H, CH_2), 6.7 (dd, J = 3 Hz, 1H, H_4 2-furyl), 7.19 (dd, J = 3 Hz, 1H, H_3 2-furyl), 7.25–7.27 (m, 2H, $H_5 + H_6$ benzimidazole), 7.45–7.47 (m, 2H, $H_4 + H_7$ benzimidazole), 7.66 (dd, J = 3 Hz, 1H, H_5 2-furyl). ^{13}C NMR (500 MHZ, DMSO-d_6): 14.82, 50.24, 110.08, 112.78, 113.61, 119.74, 123.48, 123.82, 135.91, 142.94, 144.08, 144.84, 145.87, 163.87, 165.94. IR (cm^{-1}): 1618 (C=N). MS: *m/z* 314, 2% (M^++2); *m/z* 313, 9% (M^++1); *m/z* 312, 100% (M^+); *m/z* 311, 33% (M^+-1). Anal. Calcd for $C_{15}H_{14}N_4O_2S$ (312.09): C, 57.31; H, 4.49; N, 17.82; S, 10.20. Found C, 57.37; H, 4.42; N, 17.89; S, 10.28.

4.2. Bioactivity materials and methods

4.2.1. Cytotoxicity against human breast cancer cell line MCF-7

The antitumor activity against MCF-7 was performed in the National Cancer Institute, Cancer Biology Department, Cairo, Egypt. The cytotoxicity of the synthesized compounds **3**–**11** was tested using the method of Skehan et al. [33]. Cells were plated in 96-multiwell plate (104 cells/well) for 24 h before treatment with the compounds to allow attachment of cell to wall of the plate. Different Concentrations of the compound under test (0.0, 5.0, 12.5, 25.0 and 50 μg/ml) were added to the cell monolayer. Six wells were prepared for each individual dose. Monolayer cells were incubated with the compounds for 48 h at 37 °C and in atmosphere of 5% CO_2. After 48 h cells were fixed, washed and stained with Sulforhodamine B stain. Excess stain was washed with acetic acid and attached stain was recovered with Tris EDTA buffer. Color intensity was measured in an ELISA reader. The relation between surviving fraction and drug conc. is plotted to get the survival curve of each tumor cell line after the specified compound.

4.2.2. In vitro VEGF inhibition in human breast cancer cell line MCF-7

The effect of tested compounds on the level of human vascular endothelial growth factor (VEGF) was determined utilizing human tumor cell lines including breast cancer cell line MCF-7 obtained from the American Type Culture Collection (Rockville, MD, USA). The tumor cells were maintained in Dulbecco's modified Eagle's medium (DMEM) supplemented with 10% heat inactivated fetal calf serum (GIBCO), penicillin (100 U/ml) and streptomycin (100 μg/ml) at 37 °C in humidified atmosphere containing 5% CO_2. Cells at a concentration of 0.50×10^6 were grown in a 25 cm^2 flask in 5 ml of complete culture medium.

The cells in culture medium were treated with 20 μl of IC_{50} values of the compounds or the standard reference drug, Tamoxifen dissolved in DMSO, then incubated for 24 h at 37 °C, in a humidified 5% CO_2 atmosphere. The cells were harvested and homogenates were prepared in saline using a tight pestle homogenizer until complete cell disruption.

The kit uses a double-antibody sandwich enzyme-linked immunosorbent assay (ELISA) to assay the level of human VEGF in samples. Add VEGF to monoclonal antibody enzyme well which is pre-coated with human VEGF monoclonal antibody, incubation; then, add VEGF antibodies labeled with biotin, and combined with Streptavidin-HRP to form immune complex; then carry out incubation and washing again to remove the uncombined enzyme. Then add Chromogen solution A, B, the color of the liquid changes into the blue, and at the effect of acid, the color finally becomes yellow. The chroma of color and the concentration of the human TRK of sample were positively correlated and the optical density was determined at 450 nm. The level of human VEGF in samples was calculated (ng/L) as duplicate determinations from the standard curve.

4.2.3. In vitro cyclooxygenase (COX) inhibition assay

The ability of the test compounds to inhibit ovine COX-1 and COX-2 was determined using an enzyme immunoassay (EIA) (kit catalog number 560131, Cayman Chemical, Ann Arbor, MI, USA) according to the manufacturer's instructions. Cyclooxygenase catalyzes the first step in the biosynthesis of arachidonic acid (AA) to PGH_2. $PGF_{2\alpha}$, produced from PGH_2 by reduction with stannous chloride, is measured by enzyme immunoassay (ACE™ competitive EIA). Stock solutions of test compounds were dissolved in a minimum volume of DMSO. Briefly, to a series of supplied reaction buffer solutions (960 μL, 0.1 M Tris–HCl pH 8.0 containing 5 mM EDTA and 2 mM phenol) with either COX-1 or COX-2 (10 μL) enzyme in the presence of heme (10 μL) were added 10 μL of various concentrations of test drug solutions (0, 0.01, 0.1, 1, 10 and 50 μM in a final volume of 1 mL). These solutions were incubated for a period of 5 min at 37 °C after which 10 μL of AA (100 μM) solution were added and the COX reaction was stopped by the addition of 50 μL of 1 M HCl after 2 min. $PGF_{2\alpha}$, produced from PGH_2 by reduction with stannous chloride was measured by enzyme immunoassay. This assay is based on the competition between PGs and a PG-acetylcholinesterase conjugate (PG tracer) for a limited amount of PG antiserum. The amount of PG tracer, that is, able to bind to the PG antiserum is inversely proportional to the concentration of PGs in the wells since the concentration of PG tracer is held constant while the concentration of PGs varies. This antibody–PG complex binds to a mouse anti-rabbit monoclonal antibody that had been previously attached to the well. The plate is washed to remove any unbound reagents and then Ellman's reagent, which contains the substrate to acetylcholine esterase, is added to the well.

The product of this enzymatic reaction produces a distinct yellow color that absorbs at 410 nm. The intensity of this color,

Please cite this article in press as: A. Temirak, et al., Part I. Synthesis, biological evaluation and docking studies of new 2-furylbenzimidazoles as antiangiogenic agents, European Journal of Medicinal Chemistry (2014), http://dx.doi.org/10.1016/j.ejmech.2014.01.063

determined spectrophotometrically, is proportional to the amount of PG tracer bound to the well, which is inversely proportional to the amount of PGs present in the well during the incubation: Absorbance α [Bound PG Tracer] $\alpha 1$/PGs. Percent inhibition was calculated by the comparison of compound treated to various control incubations. The concentration of the test compound causing 50% inhibition (IC_{50}, μM) was calculated from the concentration–inhibition response curve (duplicate determinations).

4.3. Molecular docking

This protocol presents a detailed outline and advice for use of AutoDock and its graphical interface, AutoDock Tools, to analyze biomolecular complexes using computational docking. The first step is to prepare the coordinate files for the docking molecule and the target molecule. The second step is the calculation of the affinity grid for the target molecule. In the third step, the docking molecule is docked with the affinity grid, and, finally, the results are analyzed.

4.3.1. Preparing the target macromolecules investigated

Our analysis to the crystal structures in the Protein Data Bank PDB comprising benzimidazole containing ligand bounded to the receptor tyrosine kinase VEGFR2 revealed 3 entries out of which we have chosen the entry with the best resolution (PDB code: 3EWH) [26] with resolution of 1.6 Å. The native ligand *N*-[4-({3-[2-(methylamino)pyrimidin-4-Yl]pyridin-2-Yl}oxy) naphthalen-1-Yl]-6-(trifluoro-methy-l)-1*H*-benzimidazol-2-amine (K11) in the co-crystallized structure downloaded from the PDB website exhibited H-bonds with the main residues in the VEGFR2: Glu885, Cys919, Lys868, Phe1047 and Asp1046. This was retrieved from the Protein Data Bank, http://www.rcsb.org/pdb/home/home.do. For each docking target, crucial amino acids of the active site were identified using data in pdbsum, http://www.ebi.ac.uk/pdbsum/.

4.3.2. Preparing a ligand file for AutoDock

The ligands are originally drawn with a widely used chemical structure drawing software. The three-dimensional structures of the aforementioned compounds were constructed using Chem3D Ultra 8.0 software [Chemical Structure Drawing Standard; Cambridge Soft corporation, USA (2003)] to obtain standard 3D structures (PDB format), then they were energetically minimized by using MOPAC with 100 iterations and minimum RMS gradient of 0.10. It is recommended to confirm whether all hydrogen atoms are in the file before working with ADT. After opening the ligand, it can be visualized and ADT now automatically computes Gasteiger charges (empirical atomic partial charges) and distinguishes between hybridization state and type of each atom. As a part of preparation, the program determines rotatable bonds of the ligand to be able to generate different conformers for the docking.

4.3.3. Setting the grid box, preparing the GRID parameter file, running AutoGrid4, and preparation of the flexible residue file

The grid parameter file tells AutoGrid4 which receptor to compute the potentials around, the types of maps to compute and the location and extent of those maps. In general, one map is calculated for each atom type in the ligand plus an electrostatics map and a separate desolvation map. The types of maps depend on the types of atoms in the ligand. Thus one way to specify the types of maps is by choosing a ligand. The grid maps of $60 \times 60 \times 60$ grid points, centered on the ligands of the complex structures, were used to cover the binding pockets. A spacing of 0.375 Å was set centered at 14.078, −5.106 and 8.682 Å, respectively for VEGFR2 kinase (PDB code: 3EWH), that encompassed the active site where the co-crystallized ligand (K11) was embedded, was used to guide the docked inhibitors within PTK receptor, and flexible residues: Glu885, Cys919, and Asp1046. Once those parameters were set in one file, AutoGrid calculates grid parameter files for each type of atom within a given area.

4.3.4. Preparing the docking parameter file and running AutoDock4

The docking parameter file tells AutoDock which map files to use, the ligand molecule to move, what its center and number of torsions are, where to start the ligand, the flexible residues to move where side chain motion in the receptor is to be modeled, which docking algorithm to use and how many runs to do. It usually has the file extension, ".dpf". Four different docking algorithms are currently available in AutoDock: SA, the original Monte Carlo simulated annealing; GA, a traditional Darwinian genetic algorithm; LS, local search; and GALS (Lamarckian genetic algorithm), which is a hybrid genetic algorithm with local search. Each search method has its own set of parameters, and these must be set before running the docking experiment itself. These parameters include what kind of random number generator to use, step sizes, *etc.* The most important parameters affect how long each docking will run. In GALS, the number of energy evaluations and the number of generations affect how long a docking will run. ADT lets you change all of these parameters, and others not mentioned here. In our study, we used AutoDock 4.2 to check the binding conformations of the synthesized compounds into the entitled VEGFR2 kinase more accurately. Lamarckian genetic algorithm was used for all molecular docking simulations. Population size of 300, mutation rate of 0.02, and crossover rate of 0.8 were set as the parameters. Simulations were performed using up to 2.5 million energy evaluations with a maximum of 27,000 generations. Each simulation was performed 10 times, yielding 10 docked conformations. The lowest energy conformations were regarded as the binding conformations between the ligands and the proteins.

4.3.5. Analyzing the docking results

Reading a docking log or a set of docking logs is the first step in analyzing the results of docking experiments. During its automated docking procedure, AutoDock outputs a detailed record to the result file has the extension ".dlg". The output includes many details about the docking which are output as AutoDock parses the input files and reports what it finds. After completing the runs, AutoDock begins an analysis phase and records details of that process. At the very end, it reports a summary of the amount of time taken and the words 'Successful Completion'. The key results in a docking log are the docked structures found at the end of each run, the energies of these docked structures and their similarities to each other. The similarity of docked structures is measured by computing the root-mean-square-deviation, RMSD, between the coordinates of the atoms. The docking results consist of the PDBQT of the Cartesian coordinates of the atoms in the docked molecule, along with the state variables that describe this docked conformation and position. As a result of AutoDock calculations we obtain the output file with in our case ten conformers of the protein-ligand complex with flexible residues and the ligand located within the binding pocket. Each structure are scored and ranked by the program by the calculated interaction energy.

Acknowledgment

The authors are grateful to the National Cancer Institute, Cancer Biology Department, Cairo, Egypt, to perform the antitumor activity against MCF-7 cancer cell lines. Deep thanks are expressed to the ' Science & Technology Development Fund' for financially supporting the manuscript through the fund of the STDF project No 1517.

Please cite this article in press as: A. Temirak, et al., Part I. Synthesis, biological evaluation and docking studies of new 2-furylbenzimidazoles as antiangiogenic agents, European Journal of Medicinal Chemistry (2014), http://dx.doi.org/10.1016/j.ejmech.2014.01.063

Appendix A. Supplementary data

Supplementary data related to this article can be found at http://dx.doi.org/10.1016/j.ejmech.2014.01.063.

References

[1] J. Folkman, Natural Medicines 1 (1995) 27–31.
[2] R.S. Kerbel, Carcinogenesis 21 (2005) 505–515.
[3] (a) P. Carmeliet, Natural Medicines 9 (2003) 653–660;
(b) A.F. Karamysheva, Biochemistry 73 (2008) 751–762.
[4] N. Ferrara, Nature Reviews Cancer 2 (2002) 795–803.
[5] S. Javerzat, P. Auguste, A. Bikfalvi, Trends in Molecular Medicine 8 (2002) 483–489.
[6] H. Cruijsen, G. Giaccone, K. Hoekman, International Journal of Cancer 118 (2006) 883–888.
[7] M. Wyler von Ballmoos, Z. Yang, J. Völzmann, I. Baumgartner, C. Kalka, S. Di Santo, PloS One 5 (2010) e14107.
[8] H.J. Kwak, J.N. So, S.J. Lee, I. Kim, G.Y. Koh, FEBS Letters 448 (1999) 249–253.
[9] P. Carmeliet, Oncology 69 (2005) 4–10.
[10] A.K. Olsson, A. Dimberg, J. Kreuger, L. Claesson–Welsh, Nature Reviews Molecular Cell Biology 7 (2006) 359–371.
[11] W. Liu, N. Reinmuth, O. Stoeltzing, A.A. Parikh, F. Fan, S.A. Ahmad, Y.D. Jung, L.M. Ellis, Seminars in Oncology 29 (2002) 96–103.
[12] A. Husain, M. Rashid, M. Shaharyar, A.A. Siddiqui, R. Mishra, European Journal of Medicinal Chemistry 62 (2013) 785–798.
[13] J.L. Wang, J. Zhang, Z.M. Zhou, Z.H. Li, W.Z. Xue, D. Xua, L.P. Hao, X.F. Han, F. Fei, T. Liu, A.H. Liang, European Journal of Medicinal Chemistry 49 (2012) 183–190.
[14] Y. Li, C. Tan, C. GÅ, C. Zhang, X. Luan, X. Chen, H. Liu, Y. Chen, Y. Jiang, Bioorganic & Medicinal Chemistry 19 (2011) 4529–4535.
[15] A. Hori, Y. Imaeda, K. Kubo, M. Kusaka, Cancer Letters 183 (2002) 53–60.
[16] K. Frazier, E. Jazan, C.M. McBride, S. Pecchi, P.A. Renhowe, C.M. Shafer, C. Taylor, D. Bussiere, M.M. He, J.M. Jansen, G. Lapointe, S. Ma, J. Vora, M. Wiesmann, Bioorganic & Medicinal Chemistry 16 (2006) 2247–2251.
[17] C.M. McBride, P.A. Renhowe, C. Heise, J.M. Jansen, G. Lapointe, S. Ma, R. Piñeda, J. Vora, M. Wiesmann, C.M. Shafer, Bioorganic & Medicinal Chemistry 16 (2006) 3595–3599.
[18] A. Viger, P.B. Dervan, Bioorganic & Medicinal Chemistry 14 (2006) 8539–8549.
[19] K. Lin, J. Lien, C. Chung, S. Kuo, T. Huang, European Journal of Pharmacology 630 (2010) 53–60.
[20] H.L. Kuo, J.C. Lien, C.H. Chung, C.H. Chang, S.C. Lo, I.C. Tsai, H.C. Peng, S.C. Kuo, T.F. Huang, Naunyn-Schmiedeberg's Archives of Pharmacology 381 (2010) 495–505.
[21] S. Huang, J. Lien, S. Kuo, T. Huang, Carcinogenesis 33 (2012) 1022–1030.
[22] K.L. Blackwell, Z.A. Haroon, S. Shan, W. Saito, G. Broadwater, C.S. Greenberg, M.W. Dewhirst, Clinical Cancer Research 11 (2000) 4359–4364.
[23] F.L. Queiroga, I. Pires, M. Parente, H. Gregório, C.S. Lopes, Veterinary Journal 189 (2011) 77–82.
[24] G. Wu, J. Luo, J.S. Rana, R. Laham, F.W. Sellke, J. Li, Cardiovascular Research 69 (2006) 512–519.
[25] D.P. Toomey, J.F. Murphy, K.C. Conlon, Surgeon 3 (2009) 174–180.
[26] V.J. Cee, A.C. Cheng, K. Romero, S. Bellon, C. Mohr, D.A. Whittington, A. Bak, J. Bready, S. Caenepeel, A. Coxon, H.L. Deak, J. Fretland, Y. Gu, B.L. Hodous, X. Huang, J.L. Kim, J. Lin, A.M. Long, H. Nguyen, P.R. Olivieri, V.F. Patel, L. Wang, Y. Zhou, P. Hughes, S. Geuns–Meyer, Bioorganic & Medicinal Chemistry Letters 19 (2009) 424–427.
[27] Y. Ozkay, Y. Tunali, H. Karaca, I. Işikda&gbreve, European Journal of Medicinal Chemistry 45 (2010) 3293–3298.
[28] V.P. Devmurari, P. Shivanand, M.B. Goyani, N.P. Jivani, International Journal of ChemTech Research 2 (2010) 681–689.
[29] H. Xiangming, M. Huiqiang, W. Yulu, Arkivoc 13 (2007) 150–154.
[30] S.R. Dhol, P.M. Gami, R.C. Khunt, A.R. Parikh, E-Journal of Chemistry 1 (2004) 228–230.
[31] V. Padmavathi, G.S. Reddy, A.V.N. Mohan, K. Mahesh, Arkivoc 17 (2008) 48–60.
[32] H.A. Saad, N.A. Osman, A.H. Moustafa, Molecules 16 (2011) 10187–10201.
[33] P. Skehan, R. Storeng, D. Scudiero, A. Monks, Journal of the National Cancer Institute 82 (1990) 1107–1112.
[34] E.V. Emile, A.D. Patricia, Marcel Dekker Inc, New York, 2001, pp. 1–8.
[35] M. Höckel, P. Vaupel, Journal of the National Cancer Institute 93 (2001) 266–276.
[36] R. Wang, Y. Lu, S. Wang, Journal of Medicinal Chemistry 46 (2003) 2287–2303.
[37] D.D. Dischino, M.J. Welch, M.R. Kilbourn, M.E. Raichle, Journal of Nuclear Medicine 24 (1983) 1030–1038.
[38] CambridgeSoft Corporation, ChemDraw, 2002. Cambridge. MA 02140 USA.

Please cite this article in press as: A. Temirak, et al., Part I. Synthesis, biological evaluation and docking studies of new 2-furylbenzimidazoles as antiangiogenic agents, European Journal of Medicinal Chemistry (2014), http://dx.doi.org/10.1016/j.ejmech.2014.01.063